ACS APPLIED MATERIALS & INTERFACES

Research Article

www.acsami.org

Responsive Stabilization of Nanoparticles for Extreme Salinity and High-Temperature Reservoir Applications

Mikhil Ranka, Paul Brown, and T. Alan Hatton*

Department of Chemical Engineering, Massachusetts Institute of Technology, Cambridge, Massachusetts 02139, United States

Supporting Information

ABSTRACT: Colloidal stabilization of nanoparticles under extreme salinity and high temperature conditions is a key challenge in the development of next generation technologies for subsurface reservoir characterization and oil recovery. Polyelectrolytes have been investigated as nanoparticle stabilizers, but typically fail at high ionic strengths and elevated temperatures due to excessive charge screening and dehydration. We report an approach to nanoparticle stabilization that overcomes these limitations, and exploits the antipolyelectrolyte phenomenon, in which screening of intrachain electrostatic interactions causes a polyzwitterion chain to undergo a structural transition from a collapsed globule to a more open coil-like regime with increases in ionic strength and temperature. Small-angle neutron scattering on a model zwitterionic polymer in solution indicated an increase in both radius of gyration and excluded volume parameter of the polymer with increases in ionic strength and temperature. The model zwitterion was subsequently incorporated within a polymeric stabilizer for nanoparticles under harsh reservoir conditions, and used to functionalize hydrophilic (silica) as well as hydrophobic (polystyrene) nanoparticles. Long-term colloidal stability was achieved at salt concentrations up to 120 000 mg/dm^3 at 90 °C, approximately twice the stability limit previously reported in the literature. The approach can be broadly generalized to a large class of synthetic polyzwitterions, and can be adapted to a wide variety of other colloidal systems in which demands placed by extreme salinity and temperature conditions must be met.

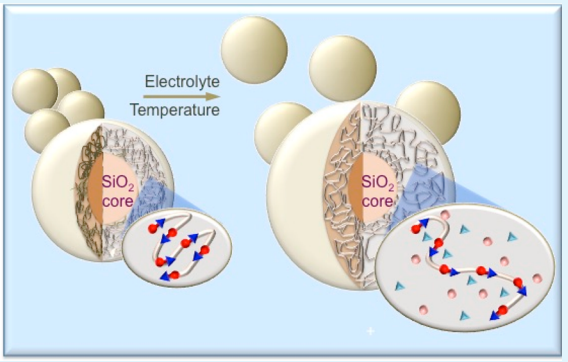

KEYWORDS: *nanoparticles, colloidal stability, enhanced oil recovery, antipolyelectrolyte effect, zwitterionic polymers, polyampholytes*

INTRODUCTION

Crude oil is the most importance source of hydrocarbon fuel today, and it is estimated that worldwide consumption will double by 2030.[1] The production of oil from subsurface reservoirs can be enhanced through exploitation of the unique properties of nanomaterials such as particles, emulsions, and gels to improve both oil field characterization and recovery.[2−5] Promising gains have been made in reservoir imaging, wettability alteration, and mobility control by the use of such nanomaterials, and there is significant potential for the development of nanoreporters that can detect stranded oil pockets, detect reservoir specific compounds and map well connectivity.[6−8] Nanoparticles, in particular, are an attractive platform for such functions because they are an order of magnitude smaller than the smallest pore throat (typically 1−10 μm) and have unique transport behavior.[9]

The main challenge in utilizing nanoparticles is that they must maintain colloidal stability under reservoir conditions of extreme salinity and high temperature. Typical salinities range from 30 000−215 000 ppm (monovalent and divalent ions), while temperatures range from 40 to 150 °C.[10] Previous strategies to ensure nanoparticles remain unaggregated have focused on developing polymer coatings that impart steric, electrostatic or electrosteric stability. Polyelectrolytes such as poly(acrylic acid), poly(vinylpyridine) and poly(styrenesulfonate) provide moderate stability, but can be susceptible to changes in pH, ionic strength, and elevated temperatures.[11−15] High ionic strengths lead to charge screening, whereas elevated temperatures disrupt favorable hydrogen bonding; both lead to reduced polymeric hydration, and eventually nanoparticle flocculation.

The most promising approaches to date have relied on strongly anionic polysulfonates that are known to remain moderately hydrated at high ionic strengths. Bagaria et al., reported an amine functionalized iron oxide core (for reservoir imaging) modified by the covalent attachment of an anionic polymer of 2-acrylamido-2-methylpropanesulfonate (AMPS) via multiple acrylic acid sites.[16] The primary nanoparticles, however, were clustered moderately in API Brine (8% NaCl + 2% $CaCl_2$ by weight) at 90 °C, and colloidal stability was not tested in brines containing significantly higher concentrations of divalent ions such as Ca^{2+} and Mg^{2+}. Divalent ions are known to be problematic, because they sharply reduce polymeric hydration via specific ion complexation.[17] In a

Received: May 17, 2015
Accepted: August 17, 2015
Published: August 17, 2015

ACS Publications © 2015 American Chemical Society

DOI: 10.1021/acsami.5b04200
ACS Appl. Mater. Interfaces 2015, 7, 19651−19658

different approach, Hwang et al., reported a carbon black nanoreporter (for detecting stranded oil pockets) to which a partially sulfonated poly(vinyl alcohol) was covalently conjugated via ester linkages.[18] However, reliance of the functionalization on hydrolysis-prone ester linkages limited the nanoreporter to use in low temperature reservoirs.

An extension of the range of temperatures and salinities to which such systems can be exposed without fear of suspension destabilization or chemical degradation would be a key advance in enabling the utilization of nanoparticles for a variety of subsurface applications. We report polymeric coatings that provide the desired long-term colloidal stability to nanoparticles under significantly harsher reservoir conditions than previously reported, and, in fact, improve in their function with increasing harshness of the reservoir environment (brine compositions are listed in Table S1). The novel coatings are based on polyampholytes, polymers that contain both positive and negative ionic groups as part of their backbone.[19] They are classified as either balanced, where the anionic and cationic groups are stoichiometric (zwitterionic), or unbalanced, where anionic and cationic units are unequal in number. Their conformation is strongly dependent on charge distribution, monomer composition and electrolyte concentration.

In contrast to polyelectrolytes that undergo a decrease in excluded volume upon addition of salt, polyampholytes can display antipolyelectrolyte behavior by undergoing an increase in excluded volume when salinity of the medium is increased.[20−22] In other words, a polyelectrolyte shrinks, while a polyampholyte swells as a function of increasing ionic

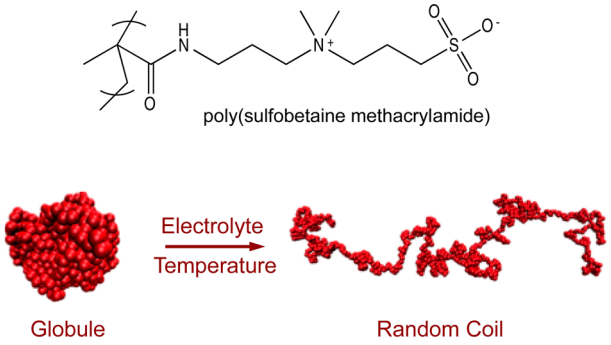

Figure 1. Coil expansion in poly(sulfobetaine methacrylamide) via electrolyte and temperature modulation.

strength (Figure 1). The scaling of size with shape and degree of polymerization for a typical polymer is

$$R_g \approx N^{\nu} \quad (1)$$

where R_g is the radius of gyration, N is the degree of polymerization, and ν is the excluded volume parameter.[23] Typical values of ν (1/3, 1/2, 3/5, and 1) are representative of globular, Gaussian, swollen and rigid rod shapes, respectively. The antipolyelectrolyte phenomenon originates from the screening of intrachain Coulombic interactions that occur upon addition of electrolyte(s) to a polyampholyte solution.[24] The reduced Coulombic interaction causes the polymer chain to swell osmotically, leading to increases in its second virial coefficient, hydrodynamic size, intrinsic viscosity and radius of gyration.[25−28] Similarly, temperature-induced expansion is observed in polyzwitterions that have a well-defined upper critical solution temperature (UCST). Because antipolyelectrolyte behavior is osmotically opposite to that of conventional polyelectrolytes, it can be utilized to develop steric stabilizers that improve rather than deteriorate in their function under increasingly challenging conditions. In other words, stabilizers can be developed that expand rather than contract in response to increasing salinity and temperature. Such responsive colloidal stabilization is illustrated schematically in Figure 2.

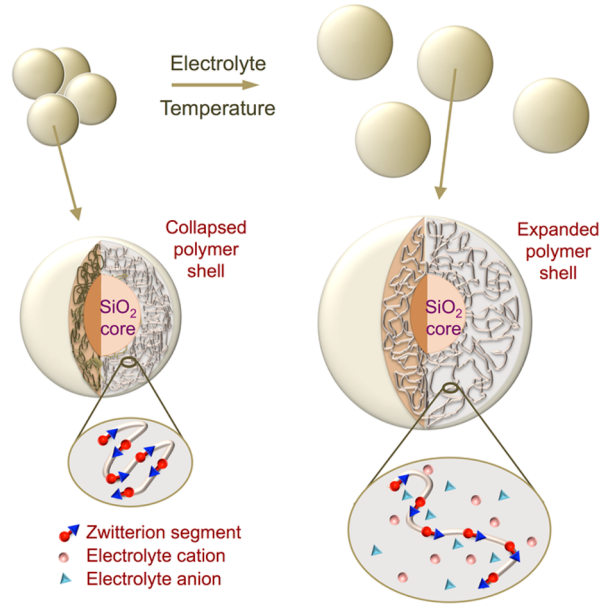

Figure 2. Responsive colloidal stabilization via polyzwitterion based graft polymer with increasing salinity and temperature. The polymer shell is shown to expand with addition of salt.

In this study, we have utilized sulfobetaine methacrylamide (SBMA), a hydrolysis resistant zwitterionic monomer that has pH invariant anionic (sulfonate) and cationic (quaternary ammonium) groups, to stabilize nanoparticle suspensions (Figure 1). Small-angle neutron scattering (SANS) was used to probe the conformational changes in poly(SBMA) that occur with changes in salt conditions (concentration and type), temperature and polymer molecular weight for a series of low polydispersity homopolymers synthesized via reversible addition−fragmentation chain transfer (RAFT) polymerization. Two copolymer architectures (random and block) incorporating the zwitterionic monomer were designed and evaluated for the stabilization of silica and polystyrene nanoparticles under harsh reservoir conditions.

MATERIALS AND METHODS

Methacrylic acid (99%) (MA), SBMA (96%), 4,4′-azobis(4-cyanovaleric acid) (ACPA), (3-aminopropyl)trimethoxysilane (97%) (APTMS), *N*-(3-(dimethylamino)propyl)-*N*′-ethylcarbodiimide hydrochloride (crystalline) (EDC), *N*-hydroxysuccinimide (98%) (NHS), and Ludox AS-40 Silica were purchased from Sigma-Aldrich USA and used without further purification. The chain transfer agent 4-Cyano-4 phenylcarbonothioylthio)pentatonic acid (CPP) was purchased from Strem Chemicals and used without further purification. Amine functionalized polystyrene nanoparticles (28 nm) were purchased from Life Technologies USA. Salts were purchased from Sigma-Aldrich USA at the following purity levels: NaCl (99%), $CaCl_2.6H_2O$ (98%), $MgCl_2.6H_2O$ (99%), Na_2SO_4 (99%), $NaHCO_3$ (99.7%), KCl (99%), KBr (99%). A 1260 Agilent gel permeation chromatograph was used to determine the molecular weight

DOI: 10.1021/acsami.5b04200
ACS Appl. Mater. Interfaces 2015, 7, 19651−19658

distribution in combination with a Wyatt miniDAWN TREOS for static light scattering. A Brookhaven 90Plus PALS was used for dynamic light scattering and a CONTIN algorithm was used to analyze autocorrelation functions. While all samples were long-term heat aged at 90 °C, measurements were made up to 65 °C due to machine limitations. Small-angle neutron scattering measurements were done at the National Institute of Standards and Technology (NIST) in Gaithersburg, MD.

Polymer Synthesis. *Homopolymer.* Molar ratios were varied from 50:1:0.25 to 400:1:0.25 ([M]:[I]:[CTA]) to tune the degree of polymerization. Initial monomer concentration was maintained at 1.5M. A typical synthesis was as follows: 20 mM of SBMA, 0.4 mM of CPP, and 0.1 mM of ACPA were dissolved in 0.5 M NaCl to a volume of 13.3 mL in a round-bottom flask. Nitrogen was bubbled through the solution for 30 min, and the reactor was heated to 60 °C. The polymerization was terminated after 24 h by exposure to atmospheric oxygen. The product was recovered via precipitation in acetone.

Random Copolymer. 25 mM of SBMA, 5 mM of MA and 0.3 mM of potassium persulfate were dissolved in 22 mL of deionized water in a round-bottom flask. Nitrogen was bubbled through the solution for 30 min, and the reactor was heated to 80 °C. The polymerization was terminated after 6 h, by exposure to atmospheric oxygen. The shorter reaction time relative to that used for the homopolymer was due to the higher temperature at which the polymerization was conducted. The product was recovered via precipitation in acetone.

Block Copolymer. A small MA block (anchor block of 20 units) was synthesized and used as a macromolecular chain transfer agent for subsequent polymerization of an SBMA block of varying lengths. Anchor Block: 10 mM of methacrylic acid and 0.5 mM of CPP were dissolved in 6.9 mL of isopropanol in a 25 mL round-bottom flask. 0.1 mM of ACPA was dissolved in 0.5 mL of methanol and added to the solution. Nitrogen was bubbled through the solution for 30 min, and the mixture was heated to 60 °C. The polymerization was again terminated after 24 h by exposure to atmospheric oxygen. The resulting solution was noted to be moderately viscous. The polymer was precipitated with diethyl ether. Stabilizer Block: Molar ratios were varied from 50:1:0.25 to 400:1:0.25 ([M]:[I]:[CTA]) respectively to tune the degree of polymerization. Initial monomer concentration was maintained at 1.5M. An example synthesis is as follows: 20 mM of SBMA, 0.4 mM of anchor block polymer, and 0.1 mM ACPA were dissolved in 0.5 M NaCl to a volume of 13.3 mL in a round-bottom flask. Nitrogen was bubbled through the solution for 30 min, and the reactor was heated to 60 °C. The polymerization was terminated after 24 h by exposure to atmospheric oxygen.

Small-Angle Neutron Scattering. SANS measurements were performed on the NG-3 (30 m) beamline at the National Institute of Standards and Technology (NIST) in Gaithersburg, MD. Neutrons with a wavelength of 6 Å were selected, and three sample detector distances were used to probe a range of wave vectors between 0.004 and 0.4 $Å^{-1}$. Data normalization using accepted procedures gave the absolute cross section $I(Q)$ (cm^{-1}) as a function of momentum transfer Q ($Å^{-1}$). Samples were prepared using D_2O (scattering length density $\rho = 6.33 \times 10^{10}$ cm^{-2}) to provide the necessary contrast and were placed in Hellma fused silica cuvettes of path length 2 mm. A concentration of 2.5% (w/w) was chosen for all the samples. Data were analyzed in absolute units ($I(Q)/cm^{-1}$) with fitted scale factors consistent with expectations based on sample compositions. Data were analyzed via the polymer excluded volume (PEV) model, as well as via Porod and Zimm approximations.[29,30]

Nanoparticle Functionalization. *Amine Functionalization of Silica Nanoparticles.* Two grams of Ludox TM-40 was washed with 50 mL of ethanol and subsequently centrifuged at 16 128 RCF for 30 min. The washing and centrifugation process was repeated to obtain 20 nm silica nanoparticles dispersed in ethanol. This dispersion was treated with 0.300 mL of APTMS at 30 °C overnight to obtain amine-decorated nanoparticles. The nanoparticles were separated from excess APTMS by two ethanol washing and centrifugration cycles. The particles were finally dispersed in 40 mL of water at pH 5 for a concentration of 2% w/v. Polymer grafting: 3 g of synthesized block copolymer was dissolved in 15 mL of water, and 2.5 mL of amine-functionalized silica/polystyrene was added dropwise with stirring at 30 °C. Subsequently, 0.6 g of EDC was added to the reaction mixture. The pH was adjusted to 4.5 and the reaction was allowed to continue overnight. The polymer-functionalized nanoparticles were separated from free polymer via centrifugation, and finallydispersed in the brine of choice at a concentration of 0.5% w/v. (DI water, synthetic seawater, Arab D brine).

RESULTS AND DISCUSSION

Polybetaines are a unique subclass of polyampholytes that exhibit distinctly different properties from those of conventional anionic or cationic polyelectrolytes. In contrast to most polyampholytes, whose spatial distribution of cationic and anionic groups is typically random, polybetaines bear an equal number of cationic (quaternary ammonium) and anionic (sulfonate) groups whose spatial distribution is defined monomerically.

Low polydispersity poly(SBMA) was synthesized using CPP as the chain transfer agent. Chain lengths of 50, 100, 150, 200, 250, 300, and 400 were targeted, with excellent control over the entire range of polymerization conditions. A slight loss of living character was observed at the higher chain lengths, but was mostly avoided by ensuring appropriate conditions to prevent aminolysis and hydrolysis of the chain transfer agent.[31−33] Polydispersities are reported in Table 1, and overlaid chromatograms are shown in Figure S1.

Table 1. Poly(SBMA) Molecular Weight and Polydispersity Synthesized via RAFT Polymerization

sample	M_n (g/mol)	polydispersity
15K	15 680	1.006
30K	31 100	1.026
45K	47 810	1.070
60K	53 650	1.126
75K	70 890	1.092
90K	89 891	1.120
120K	124 000	1.235

Small-Angle Neutron Scattering. The antipolyelectrolyte phenomenon was probed via small-angle neutron scattering (SANS), which was used to determine the radii of gyration (R_g) and excluded volume parameters (ν) for 15K, 45K, 75K, and 120K homopolymers under the extreme conditions of salinity and temperatures representative of subsurface reservoirs. The phase behavior of polybetaines has been accepted to follow a simple Flory−Huggins model[24]

$$K_B T\chi = \varepsilon_{ms} - 0.5[\varepsilon_{mm} + \varepsilon_{ss}] \quad (2)$$

where χ is the interaction parameter and ε_{ms}, ε_{mm}, and ε_{ss} are the monomer−solvent, monomer−monomer, and solvent−solvent contact energies, respectively. Contact energies are sensitive to the Debye length, and solvent quality, which can be modulated through the electrolyte concentration and temperature. The effects of these solution conditions on polymer conformation are particularly evident in log−log plots in the Porod regime ($0.02 < Q < 0.05$), from which the fractal dimension of the polymer can be obtained via the equation

$$\log I = \log A - n\log Q \quad (3)$$

where n, the Porod slope, is the inverse of the excluded volume parameter ν (i.e., $n = 1/\nu$). A slope of $n = 3$ is the signature of a globular coil, whereas a slope of $n = 5/3$ represents a fully

DOI: 10.1021/acsami.5b04200
ACS Appl. Mater. Interfaces 2015, 7, 19651−19658

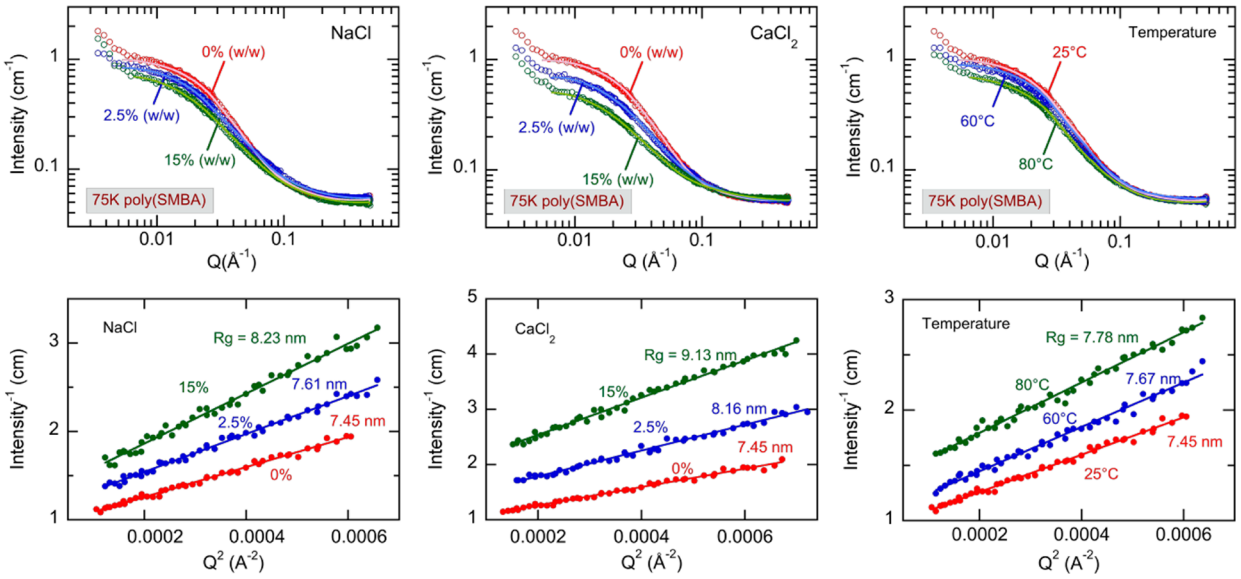

Figure 3. SANS spectra and partial Zimm plots for 75K homopolymer with varying NaCl, $CaCl_2$, and temperature.

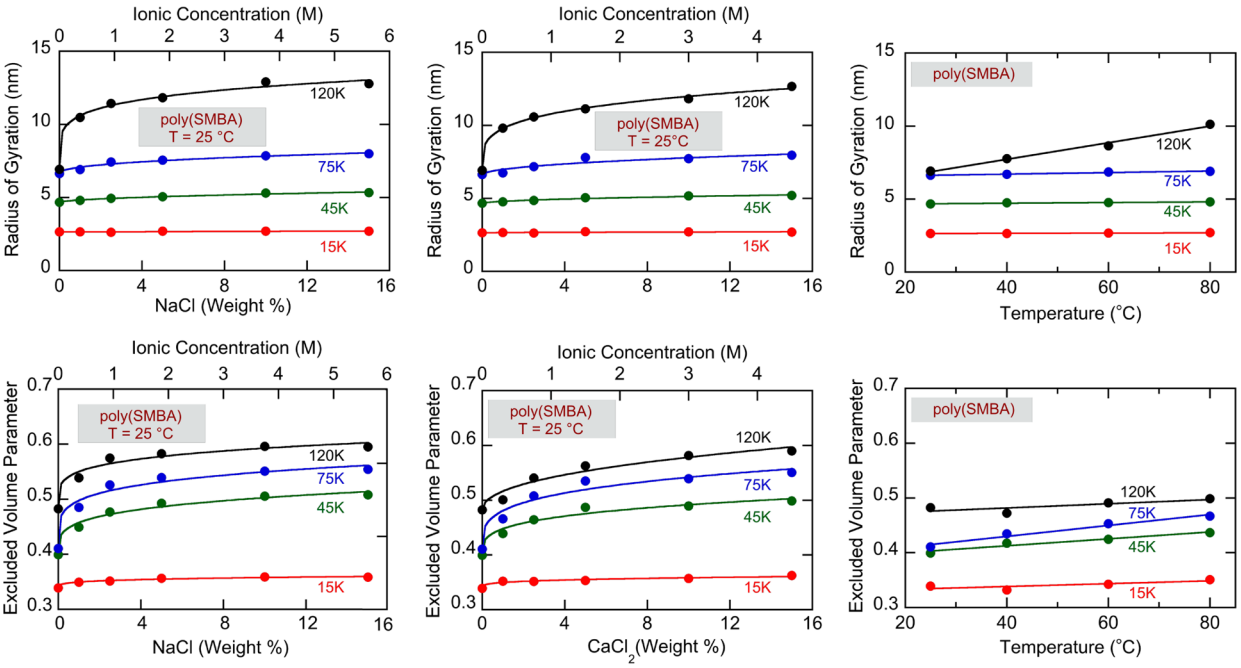

Figure 4. Dependence of radius of gyration and excluded volume parameter for poly(SMBA) of different molecular weights on salt type and concentration, and on temperature. Higher-molecular-weight polymers are more sensitive to both size and shape change.

swollen coil. Therefore, the magnitude of n is expected to decrease with improvements in solvent quality. This trend was indeed observed and example log–log plots for the 75K homopolymer are shown in Figure 3; Porod fit parameters are tabulated in Table S2–S4.

The excluded volume parameter was observed to be $\nu \approx 0.41$ with no added salt, at a temperature of 25 °C, and increased to a maximum value of $\nu \approx 0.56$ upon addition of NaCl or $CaCl_2$. Temperature was noted to have a similar but weaker effect, with ν increasing from ∼0.41 to ∼0.48 over the range examined. Additionally, partial Zimm plots were used to quantify changes in R_g as a function of electrolyte concentration, type and temperature. A Lorentzian form for the Q dependence of scattering intensity was assumed[30]

$$I(Q) = \frac{I_o}{1 + Q^2\xi^2} \tag{4}$$

In the low Q region, $\xi = R_g/\sqrt{3}$, and a plot of I^{-1} vs Q^2 allows the correlation length ξ to be estimated. Partial Zimm plots for the 75K homopolymer are shown in Figure 3, and the results are tabulated in Table S5–S7.

A polymer excluded volume model with form factor:

$$P(Q) = 2\int (1 - x)\exp\left[-\frac{Q^2a^2}{6}N^{2\nu}x^{2\nu}\right] \tag{5}$$

where a is the chain statistical segment (Kuhn) length and N is degree of polymerization, was also used to fit the scattering profiles for all four molecular weight polymers across the entire

DOI: 10.1021/acsami.5b04200
ACS Appl. Mater. Interfaces 2015, 7, 19651−19658

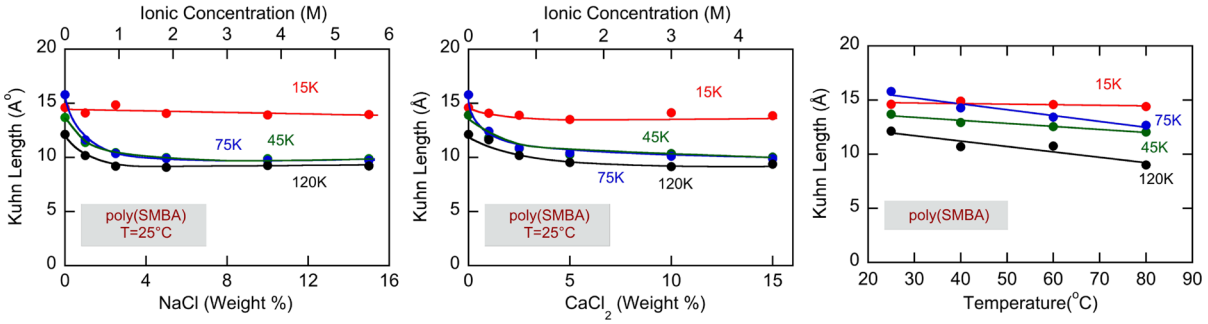

Figure 5. Dependence of Kuhn length on NaCl and $CaCl_2$ concentration, and on temperature for different molecular weights of poly(SMBA).

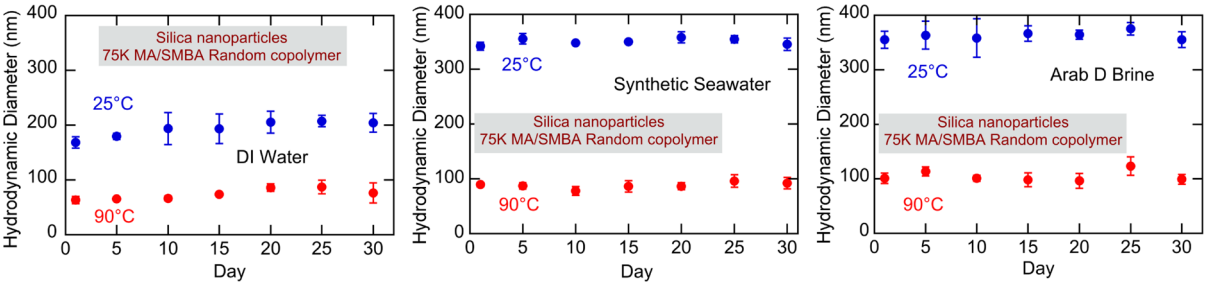

Figure 6. Colloidal stability of MA/SBMA random copolymer functionalized silica nanoparticles in three different electrolyte environments. No reversible clustering was observed, and measurements were discontinued beyond 30 days.

range of temperatures and salt concentrations examined (model fits are shown as light lines on the spectra in Figure 3).[29] The extracted model parameters were in excellent agreement with the Porod and partial Zimm fits (comparisons in Table S2–S7), and the dependence of R_g and ν on solution conditions is shown in Figure 4 and tabulated in Table S8–S13.

These results are a clear manifestation of the antipolyelectrolyte phenomenon, but perhaps the most notable feature of Figure 4 is the molecular weight dependency of the excluded volume parameter ν. At 5% NaCl, for example, ν was found to be 0.35 (globular) for 15K and 0.58 for 120K (swollen coil). These results are a departure from the scaling implied by eq 1, according to which ν is a function only of solvent quality and not of molecular weight. This scaling however is only valid in the limit of large N, since it assumes a flexible chain with a large number of Kuhn segments.[23] The Kuhn length calculated via the polymer excluded volume model of Benoit[29]

$$a = \left(\frac{R_g^2 (2\nu + 1)(2\nu + 2)}{N^{2\nu}} \right)^{1/2} \quad (6)$$

is shown in Figure 5 as a function of salt, temperature, and molecular weight.

Poly(SBMA) was determined to have a Kuhn length between $a \approx 15$ Å and $a \approx 9$ Å (depending on salt concentrations, as discussed below), and thus the number of Kuhn segments lay between ~2 (15K without added salt) to ~14 (120 K with 15 wt % $CaCl_2$). These values are clearly too low for the large N limit of eq 1 to be valid, and the decoupling between R_g and ν observed in Figure 4 is to be expected. An electrostatic contribution to a can also be anticipated since charge screening leads to a decrease in the length scale over which electrostatic interactions dominate (decrease in Debye length). This is a known phenomenon for polyelectrolytes, and the same effects were indeed observed for antipolyelectrolyte based poly(SBMA).[34,35]

It is interesting to contrast the behavior of the lower molecular weight 15K with that of the higher molecular weight polymers 45K to 120 K observed in Figures 4 and 5. The 15K homopolymer has a constant Kuhn length and an invariant globular shape, whereas the 45K–120K systems show a steady decrease in a and a clear transition toward more swollen conformations. Such a molecular weight dependence of a and ν is surprising, but can be rationalized on the basis of the average distance l between an interacting pair of ammonium and sulfonate groups confined within a polyzwitterion coil. This average spacing is known to increase with molecular weight.[24] Therefore, for a densely packed globular chain such as 15K, l is very small, and attractive ionic interactions dominate over charge screening, leading to retention of the strong globular structure and constant Kuhn length. For 45K–120 K systems on the other hand, monomeric units are less densely packed, and thus allow charge screening to dominate over electrostatic interactions. Because chain swelling is a result of reduced ionic correlations, electrolyte addition leads to a more flexible coil and a decrease in a.

Another notable feature is the relative effect of NaCl vs $CaCl_2$. While previous studies have established an order of solubilization for different salt cation and anion structures, a preferential order for R_g and ν sensitivity has not been established.[25] Figure 4 implies that the divalent Ca^{2+} is a much stronger cation than is monovalent Na^+ when compared on a cumulative ionic strength basis rather than on a mass percent basis.

Colloidal Stability. The SANS results indicate that SBMA has an osmotic response opposite that of polyelectrolytes. This is unique in the context of colloidal applications, since it enables the design of a steric layer that strengthens rather than weakens suspension stability in response to increasingly harsh reservoir conditions (Figure 2). Additionally, SBMA is an ideal monomer of choice due to its hydrophilic backbone (amide group) and hydrolytic stability (methacrylamide > acrylamide >

DOI: 10.1021/acsami.5b04200
ACS Appl. Mater. Interfaces 2015, 7, 19651–19658

methacrylate > acrylate).[20] Silica was initially chosen as the model core because of its chemical and thermal resistance to reservoir conditions.[3,9] Permanent immobilization of the polymeric layer was necessary to prevent diffusive desorption and thermal degradation of the attached polymers, and was easily accomplished via carbodiimide conjugation to the particle surface. This conjugation necessarily required incorporation of acid sites on the polymeric backbone, which was achieved by copolymerization of MA with SBMA. Because the distribution of acid sites along the polymer backbone can be expected to affect grafting density, geometry, and cumulative repulsion offered by the steric layer significantly, two polymeric architectures were designed: a free radical copolymer with randomly distributed acid sites, and a RAFT-based block copolymer with a segregated acid block.

Random Copolymer. Although the random copolymer is easily synthesized, it is inherently disadvantaged as a stabilizer because it is a hybrid of a polyelectrolyte (MA) and an antipolyelectrolyte (SBMA). The osmotic response of MA is opposite to that of SBMA, and therefore weakens the cumulative repulsion offered by the copolymer. Figure 6 shows the stability of random copolymer-functionalized silica nanoparticles in DI water, synthetic seawater and Arab D brine at two different heat-aging temperatures. Temperature dependent clustering was observed, with a smaller particle size at 90 °C and a larger particle size at 25 °C. The clustering at lower temperatures was likely due to an insufficient hydration of the SBMA units to counter the relatively poor solvation of MA in an electrolyte-rich environment. At elevated temperatures, on the other hand, increased SBMA solvation provided the necessary steric repulsion and led to deaggregation of the clusters.

Block Copolymer. To overcome the temperature dependent clustering observed with random copolymer stabilizers, we designed a block copolymer with a segregated MA anchor block. The segregation of the anchor block is useful on two accounts: it allows for a higher graft density, and for exclusion of MA from the steric layer. High graft densities are known to introduce repulsive entropic effects via stretched chain compression, while exclusion of MA from the steric layer was expected to overcome the issue of competing osmotic effects. Overlayed chromatograms of the block copolymers prepared at four different molecular weight of the SBMA block are shown in Figure S2, and polydispersities are reported in Table 2.

Table 2. MA/SBMA Block Copolymer Molecular Weight and Polydispersity Synthesized via RAFT Polymerization

sample	M_n (g/mol)	polydispersity
15K-Block	13 750	1.227
35K-Block	36 920	1.035
75K-Block	74 990	1.092
120 K-Block	124 700	1.023

Our SANS studies indicated that larger SBMA blocks (75K−120K) expand in size (R_g) and swell (ν) more compared to smaller and more globular SBMA blocks (15K−45K). Thus, 75K−120K blocks were expected to perform better as stabilizing agents, and we therefore investigated the stability of particles functionalized with the 75K-block polymer in DI water, synthetic seawater, and Arab D brine; the results are given in Figure 7. No temperature-dependent clustering was observed, and uniform long-term stability was achieved over the entire desired temperature and salt ranges.

The results shown in Figure 7 were obtained with the nanoparticles dispersed in polypropylene vials. When glass vials were used to contain the suspensions, the silica nanoparticles were found to be colloidally unstable following exposure to elevated temperatures for a week. The instability was likely due to strong interactions between the silica core and the glass vial surface, thereby providing the nanoparticles with a favorable site for adsorption and eventual aggregation. That this behavior was not observed in polypropylene vials was attributed to the surface hydrophobicity and weak interaction between the vial surface and silica core. To test this hypothesis, we functionalized a hydrophobic, amine-functionalized polystyrene core (28 nm) with the 75K-block copolymer via carbodiimide conjugation. With these particles, long-term colloidal stability was observed in both glass and polypropylene vials, indicating that the steric barrier was sufficient to overcome any interaction with glass or polypropylene surfaces. Long-term stability results are shown in Figure 8.

The results presented above are of significant importance on three accounts. First, they demonstrate a novel utilization of the antipolyelectrolyte phenomenon for developing colloidal stabilizers that actually strengthen in their performance with increasing harshness of reservoir conditions. Second, there are a large number of synthetic polybetaines that could be engineered similarly to serve as polymeric stabilizers, thereby extending the design space for utilizing the antipolyelectrolyte effect in the stabilization of nanoparticle suspensions. Third, and most importantly, it significantly extends the range of electrolyte concentrations over which long-term colloidal stability can be achieved for reservoir applications. To the best of our knowledge, no other studies have reported successful long-term stabilization in Arab D or equivalently harsh brine. Furthermore, the coating shows excellent stability at significantly higher concentrations of Mg^{2+} and Ca^{2+} than has been previously reported.

CONCLUSIONS

We have overcome the key deficiency of polyelectrolyte-based colloidal stabilization in strong brines (double layer collapse), by designing antipolyelectrolyte based stabilizers that advantageously utilize the enhanced charge screening afforded by harsh reservoir conditions. The effect was quantified using SANS for a series of low polydispersity homopolymers of poly(sulfobetaine methacrylamide) prepared via RAFT polymerization, and significant molecular weight dependencies on size and shape were observed. The larger sized polymers (75K-120 K) were noted to be optimal for stabilizing nanoparticles under harsh reservoir conditions, and successful stabilization was achieved under significantly harsher conditions (including at high concentrations of divalent ions) than previously reported. Additionally, the approach proved to be versatile in terms of the being applicable to hydrophilic as well as hydrophobic nanoparticles.

There is broad scope for the design of similar coatings for cores such as iron oxide, graphene and up-conversion nanocrystals (UCN's), thereby enabling development of next generation technologies for reservoir imaging, well tracing, and temporal temperature mapping. The antipolyelectrolyte stabilization concept can also be extended to other colloidal systems such as nanoemulsions and gels, as well as environmental remediation catalysts that require nanoparticle stability in high

DOI: 10.1021/acsami.5b04200
ACS Appl. Mater. Interfaces 2015, 7, 19651−19658

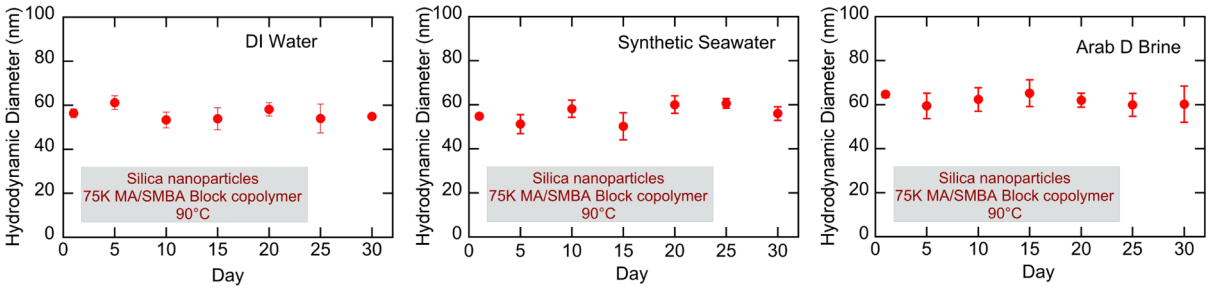

Figure 7. Colloidal stability of MA/SBMA block copolymer functionalized silica nanoparticles in three different electrolyte environments at 90 °C. No reversible clustering was observed, and measurements were discontinued beyond 30 days.

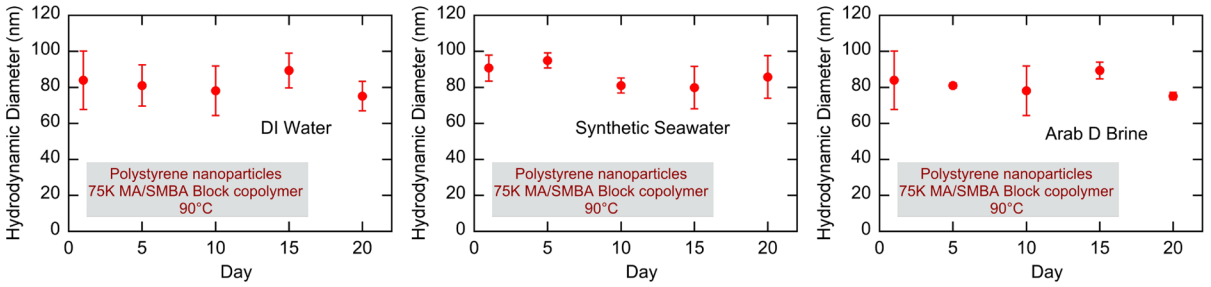

Figure 8. Colloidal stability of MA/SBMA block copolymer functionalized polystyrene nanoparticles in three different electrolyte environments at 90 °C.

ionic strength solutions.[36] Overall, polyzwitterionics have been demonstrated to address the key challenge of stabilizing nanoparticles for subsurface applications successfully, and hold immense promise for serving as a future platform for the development of a wide range of applications, including nanoreporting, wettability control, and mobilization of stranded oil pockets.

■ ASSOCIATED CONTENT

Supporting Information

The Supporting Information is available free of charge on the ACS Publications website at DOI: 10.1021/acsami.5b04200.

Chromatogram traces from RAFT polymerizations; SANS data for R_g and ν for the various molecular weights examined (PDF)

■ AUTHOR INFORMATION

Corresponding Author

*E-mail: tahatton@mit.edu.

Notes

The authors declare no competing financial interest.

■ ACKNOWLEDGMENTS

This work was supported by Saudi Aramco under the MIT Energy Initiative. We thank Hari Katepalli for his assistance with the analysis of the SANS results.

■ REFERENCES

(1) *Annual Energy Consumption Projection Report 2013*; U.S. Energy Information Administration: Washington, D. C., 2013.

(2) Turkenburg, D.; Chin, P. T. K.; Fischer, H. Use of Modified Nanoparticles in Oil and Gas Reservoir Management. *Soc. Pet. Eng.* **2012**, DOI: 10.2118/157120-MS.

(3) Kong, X.; Ohadi, M. Applications of Micro and Nano Technologies in the Oil and Gas Industry - Overview of the Recent Progress. *Soc. Pet. Eng.* **2010**, DOI: 10.2118/138241-MS.

(4) Zhang, T.; Roberts, M.; Bryant, S. L.; Huh, C. Foams and Emulsions Stabilized With Nanoparticles for Potential Conformance Control Applications. *Soc. Pet. Eng.* **2009**, DOI: 10.2118/121744-MS.

(5) Agenet, N.; Moradi-Tehrani, N.; Tillement, O. Fluorescent Nanobeads: A New Generation of Easily Detectable Water Tracers. *Int. Petro. Technol. Conf.* **2011**, DOI: 10.2523/15312-MS.

(6) Zhang, T.; Davidson, D.; Bryant, S. L.; Huh, C. Nanoparticle-Stabilized Emulsions for Applications in Enhanced Oil Recovery. *Soc. Pet. Eng.* **2010**, DOI: 10.2118/129885-MS.

(7) Kini, G. C.; Yu, J.; Wang, L.; Kan, A. T.; Biswal, S. L.; Tour, J. M.; Tomson, M. B.; Wong, M. S. Salt and Temperature Stable Quantum Dot Nanoparticles for Porous Media Flow. *Colloids Surf., A* **2014**, *443*, 492−500.

(8) Shamsi Jazeyi, H.; Miller, C. A.; Wong, M. S.; Tour, J. M.; Verduzco, R. Polymer Coated Nanoparticles for Enhanced Oil Recovery. *J. Appl. Polym. Sci.* **2014**, *131* (15), 40576.

(9) Rodriguez Pin, E.; Roberts, M.; Yu, H.; Huh, C.; Bryant, S. L. Enhanced Migration of Surface-Treated Nanoparticles in Sedimentary Rocks. In *Society of Petroleum Engineers Annual Technical Conference and Exhibition*; New Orleans, LA, Oct 4−7, 2009 ; Society of Petroleum Engineers: Richardson, TX, 2009; 10.2118/124418-MS.

(10) Okasha, T. M.; Alshiwaish, A. Effect of Brine Salinity on Interfacial Tension in Arab-D Carbonate Reservoir, Saudi Arabia. *Soc. Pet. Eng.* **2009**, DOI: 10.2118/119600-MS.

(11) Caldelas, F. M.; Murphy, M.; Huh, C.; Bryant, S. L. Factors Governing Distance of Nanoparticle Propagation in Porous Media. *Soc. Pet. Eng.* **2011**, DOI: 10.2118/142305-MS.

(12) Ayatollahi, S.; Zerafat, M. Nanotechnology-Assisted EOR Techniques: New Solutions to Old Challenges. *Soc. Pet. Eng.* **2012**, DOI: 10.2118/157094-MS.

(13) Ersenkal, D. A.; Ziylan, A.; Ince, N. H.; Acar, H. Y.; Demirer, M.; Copty, N. K. Impact of Dilution on the Transport of Poly(acrylic acid) Supported Magnetite Nanoparticles in Porous Media. *J. Contam. Hydrol.* **2011**, *126* (3−4), 248−257.

(14) Yu, H.; Kotsmar, C.; Yoon, K. Y.; Ingram, D. R.; Johnston, K. P.; Bryant, S. L.; Huh, C. Transport and Retention of Aqueous Dispersions of Paramagnetic Nanoparticles in Reservoir Rocks. *Soc. Pet. Eng.* **2010**, DOI: 10.2118/129887-MS.

(15) Kim, H.; Phenrat, T.; Tilton, R. D.; Lowry, G. V. Effect of Kaolinite, Silica Fines and pH on Transport of Polymer Modified Zero

DOI: 10.1021/acsami.5b04200
ACS Appl. Mater. Interfaces 2015, 7, 19651−19658

Valent Iron Nano-Particles in Heterogeneous Porous Media. *J. Colloid Interface Sci.* **2012**, *370* (1), 1−10.
(16) Bagaria, H. G.; Xue, Z.; Neilson, B. M.; Worthen, A. J.; Yoon, K. Y.; Nayak, S.; Cheng, V.; Lee, J. H.; Bielawski, C. W.; Johnston, K. P. Iron Oxide Nanoparticles Grafted with Sulfonated Copolymers are Stable in Concentrated Brine at Elevated Temperatures and Weakly Adsorb on Silica. *ACS Appl. Mater. Interfaces* **2013**, *5* (8), 3329−3339.
(17) Sabbagh, I.; Delsanti, M. Solubility of Highly Charged Anionic Polyelectrolytes in Presence of Multivalent Cations: Specific Interaction Effect. *Eur. Phys. J. E: Soft Matter Biol. Phys.* **2000**, *1* (1), 75−86.
(18) Hwang, C.; Wang, L.; Lu, W.; Ruan, G.; Kini, G. C.; Xiang, C.; Samuel, E. G.; Shi, W.; Kan, A. T.; Wong, M. S.; Tomson, M. B.; Tour, J. M. Highly Stable Carbon Nanoparticles Designed for Downhole Hydrocarbon Detection. *Energy Environ. Sci.* **2012**, *5* (8), 8304−8309.
(19) Dobrynin, A. V.; Colby, R. H.; Rubinstein, M. Polyampholytes. *J. Polym. Sci., Part B: Polym. Phys.* **2004**, *42* (19), 3513−3538.
(20) Laschewsky, A. Structures and Synthesis of Zwitterionic Polymers. *Polymers* **2014**, *6*, 1544−1601.
(21) Polzer, F.; Heigl, J.; Schneider, C.; Ballauff, M.; Borisov, O. V. Synthesis and Analysis of Zwitterionic Spherical Polyelectrolyte Brushes in Aqueous Solution. *Macromolecules* **2011**, *44* (6), 1654−1660.
(22) Schulz, D. N.; Peiffer, D. G.; Agarwal, P. K.; Larabee, J.; Kaladas, J. J.; Soni, L.; Handwerker, B.; Garner, R. T. Phase behavior and Solution Properties of Sulphobetaine Polymers. *Polymer* **1986**, *27* (11), 1734−1742.
(23) Flory, P. J. *Principles of Polymer Chemistry*, 1st ed.; Cornell University Press: Ithaca, NY, 1953.
(24) Mary, P.; Bendejacq, D.; Labeau, M.; Dupuis, P. Reconciling Low and High Salt Solution Behavior of Sulfobetaine Polyzwitterions. *J. Phys. Chem. B* **2007**, *111* (27), 7767−7777.
(25) Muroga, Y.; Amano, M.; Katagiri, A.; Noda, I.; Nakaya, T. pH and Ionic Strength Dependences of the Intrinsic Viscosity of Betaine Type Polyampholyte. *Polym. J.* **1995**, *27* (1), 65−70.
(26) Kudaibergenov, S.; Jaeger, W.; Laschewsky, A. Polymeric Betaines: Synthesis, Characterization, and Application. *Adv. Polym. Sci.* **2006**, *201* (1), 157−224.
(27) Berlinova, I. V.; Dimitrov, I. V.; Kalinova, R. G.; Vladimirov, N. G. Synthesis and Aqueous Solution Behavior of Copolymers Containing Sulfobetaine Moieties in Side Chains. *Polymer* **2000**, *41* (3), 831−837.
(28) Liaw, D.; Huang, C.; Sang, H.; Kang, E. Aqueous Solution and Photophysical Properties of Cationic Poly(trimethyl methacrylamidophenyl ammonium methylsulfate) and Zwitterionic Poly(N,N-dimethylmethacrylamidophenyl ammonium propane sultone). *Polymer* **2001**, *42* (1), 209−216.
(29) Benoit, H. *Comptes Rendus* **1957**, *245*, 2244−2247.
(30) Hammouda, B. SANS from Homogeneous Polymer Mixtures−A Unified Overview. In *Polymer Characteristics*; Advances in Polymer Science; Springer: New York, 1993; Vol. *106*, pp 87−133, 10.1007/BFb0025862.
(31) Thomas, D. B.; Convertine, A. J.; Hester, R. D.; Lowe, A. B.; McCormick, C. L. Hydrolytic Susceptibility of Dithioester Chain Transfer Agents and Implications in Aqueous RAFT polymerizations. *Macromolecules* **2004**, *37* (5), 1735−1741.
(32) Lowe, A. B.; McCormick, C. L. Reversible Addition Fragmentation Chain Transfer (RAFT) Radical Polymerization and the Synthesis of Water Soluble (Co)polymers under Homogeneous Conditions in Organic and Aqueous Media. *Prog. Polym. Sci.* **2007**, *32* (3), 283−351.
(33) Donovan, M. S.; Lowe, A. B.; Sanford, T. A.; McCormick, C. L. Sulfobetaine Containing Diblock and Triblock Copolymers via Reversible Addition Fragmentation Chain Transfer Polymerization in Aqueous Media. *J. Polym. Sci., Part A: Polym. Chem.* **2003**, *41* (9), 1262−1281.
(34) Nierlich, M.; Boue, F.; Lapp, A.; Oberthür, R. Characteristic Lengths and the Structure of Salt Free Polyelectrolyte Solutions. A Small Angle Neutron Scattering Study. *Colloid Polym. Sci.* **1985**, *263* (12), 955−964.
(35) Spiteri, M.; Boue, F.; Lapp, A.; Cotton, J. P. Persistence Length for a PSSNa Polyion in Semidilute Solution as a Function of the Ionic Strength. *Phys. Rev. Lett.* **1996**, *77* (26), 5218−5220.
(36) Zhang, W. Nanoscale Iron Particles for Environmental Remediation: An Overview. *J. Nanopart. Res.* **2003**, *5* (3−4), 323−332.

DOI: 10.1021/acsami.5b04200
ACS Appl. Mater. Interfaces 2015, 7, 19651−19658